Journal of the American College of Cardiology Vol. 52, No. 23, 2008

Published by Elsevier Inc.
ISSN 0735-1097/08/$34.00
doi:10.1016/j.jacc.2008.08.048

Molecular Imaging of Matrix Metalloproteinase in Atherosclerotic Lesions

Resolution With Dietary Modification and Statin Therapy

Shinichiro Fujimoto, MD, PHD,* Dagmar Hartung, MD,* Satoru Ohshima, MD, PHD,* D. Scott Edwards, PHD,† Jun Zhou, MD,* Padmaja Yalamanchili, PHD,† Michael Azure, PHD,† Ai Fujimoto, MD, PHD,* Satoshi Isobe, MD, PHD,* Yuji Matsumoto, MD, PHD,* Hendricus Boersma, PHARMD, PHD,‡ Nathan Wong, PHD,* Junichi Yamazaki, MD,§ Navneet Narula, MD,* Artiom Petrov, PHD,* Jagat Narula, MD, PHD, FACC*

Irvine, California; North Billerica, Massachusetts; Groningen, the Netherlands; and Tokyo, Japan

Objectives This study sought to evaluate the feasibility of noninvasive detection of matrix metalloproteinase (MMP) activity in experimental atherosclerosis using technetium-99m–labeled broad matrix metalloproteinase inhibitor (MPI) and to determine the effect of dietary modification and statin treatment on MMP activity.

Background The MMP activity in atherosclerotic lesions contributes to the vulnerability of atherosclerotic plaques to rupture.

Methods Atherosclerosis was produced in 34 New Zealand White rabbits by balloon de-endotheliazation of the abdominal aorta and a high-cholesterol diet. In addition, 12 unmanipulated rabbits were used as controls and 3 for blood clearance characteristics. In vivo micro–single-photon emission computed tomography (SPECT) imaging was performed after radiolabeled MPI administration. Subsequently, aortas were explanted to quantitatively measure percent injected dose per gram (%ID/g) MPI uptake. Histological and immunohistochemical characterization was performed and the extent of MMP activity was determined by gel zymography or enzyme-linked immunosorbent assays.

Results The MPI uptake in atherosclerotic lesions ($n = 18$) was clearly visualized by micro-SPECT imaging; MPI uptake was markedly reduced by administration of unlabeled MPI before the radiotracer ($n = 4$). The MPI uptake was also significantly reduced after diet withdrawal ($n = 6$) and fluvastatin treatment ($n = 6$); no uptake was observed in normal control rabbits ($n = 12$). The %ID/g MPI uptake ($0.10 \pm 0.03\%$) in the atherosclerotic lesions was significantly higher than the uptake in control aorta ($0.016 \pm 0.004\%$, $p < 0.0001$). Uptake in fluvastatin ($0.056 \pm 0.011\%$, $p < 0.0005$) and diet withdrawal groups ($0.043 \pm 0.011\%$, $p < 0.0001$) was lower than the untreated group. The MPI uptake correlated with immunohistochemically verified macrophage infiltration ($r = 0.643$, $p < 0.0001$), and MMP-2 ($r = 0.542$, $p < 0.0001$) or MMP-9 ($r = 0.578$, $p < 0.0001$) expression in plaques.

Conclusions The present data show the feasibility of noninvasive detection of MMP activity in atherosclerotic plaques, and confirm that dietary modification and statin therapy reduce MMP activity. (J Am Coll Cardiol 2008;52: 1847–57) © 2008 by the American College of Cardiology Foundation

The atherosclerotic plaques vulnerable to rupture frequently show large lipid cores, positive vascular remodeling, thin fibrous caps, and inflammatory infiltrates (1–3). Significant upregulation of matrix metalloproteinase (MMP) is observed in such plaques, which is directly related to the extent of inflammation (4,5). The MMP expression and activation contributes to attenuation of fibrous caps and expansive vascular remodeling, and therefore to the vulnerability of plaque to rupture (6–9); MMP expression is only minimally observed in stable plaques (10). Diet modification and statin therapy have been shown to resolve the extent of inflammatory cell infiltration in the plaque and MMP activity (11–15). As such, MMP activity offers an important target for molecular imaging for the detection of unstable plaques and for monitoring the effects of therapeutic interventions.

From the *University of California, Irvine School of Medicine, Irvine, California; †Bristol-Myers Squibb, Medical Imaging, North Billerica, Massachusetts; ‡University Medical Center, Groningen, the Netherlands; and the §Toho University School of Medicine, Ohmori Hospital, Tokyo, Japan. The study was supported by National Institutes of Health grant RO1 (HL 078681) provided to Dr. Jagat Narula. The authors received MPI_RP805 from Bristol-Myers Squibb Imaging Co. (North Billerica, Massachusetts) and fluvastatin from Novartis and Tanabe Pharmaceuticals (Tokyo, Japan). Steven E. Nissen, MD, MACC, served as Guest Editor for this paper.

Manuscript received January 11, 2008; revised manuscript received August 12, 2008, accepted August 12, 2008.

JACC Vol. 52, No. 23, 2008
December 2, 2008:1847–57

Abbreviations and Acronyms

%ID/g = percent total injected dose per gram of tissue
CT = computed tomography
HC = high cholesterol
MMP = matrix metalloproteinase
MPI = matrix metalloproteinase inhibitor
NZW = New Zealand White
PBS = phosphate-buffered saline
SMC = smooth muscle cell
SPECT = single-photon emission computed tomography

Recently, a fluorescent MMP substrate has been used for optical imaging of atherosclerotic plaques in mice (16), which gets cleaved in the presence of active MMP expression and the fluorescent fragment is trapped to become amenable to imaging. In the present study, we used a technetium-99m–labeled matrix metalloproteinase inhibitor (MPI) that binds to a variety of active MMP family members. It has been hypothesized (17–19) that the extent of MPI uptake would offer a precise estimate of MMP activity in the atherosclerotic lesions noninvasively.

Methods

The atherosclerotic lesions were induced experimentally in New Zealand White (NZW) rabbits by balloon de-endothelialization of the abdominal aorta followed by a high-fat and high-cholesterol (HC) diet. After intravenous administration of technetium-99m–labeled MPI, noninvasive imaging of the radiotracer uptake was performed by micro–single-photon emission computed tomography (SPECT)/micro-computed tomography (CT) system. The animals were killed after in vivo imaging, and aortas were explanted for ex vivo imaging. Thereafter, the quantitative MPI uptake was determined by gamma counting of serially sectioned aortic tissue specimens. Quantitative MPI uptake was then compared with immunohistochemically verified macrophage prevalence and MMP-2 and -9 expression in the aortic specimens. The MPI uptake was also correlated with the MMP-2 and -9 activity in tissue specimens measured by enzyme-linked immunosorbent assay or by gel zymography. The impact of dietary modification and statin therapy was investigated by measuring a change in the MPI uptake in the additional groups of atherosclerotic animals.

Classification of study animals. In the present study, noninvasive radionuclide MPI imaging was performed for the detection of MMP in 49 NZW rabbits (Table 1). Of these, 34 rabbits were subjected to balloon de-endothelization of their abdominal aorta followed by 4 months of hypercholesterolemic diet for induction of experimental atherosclerotic lesions. Of the remaining 15 unmanipulated rabbits fed normal chow for 4 months, 12 were used for MPI imaging as disease controls and 3 for conducting a blood clearance study. Of the 34 atherosclerotic rabbits, 18 received an uninterrupted cholesterol diet for all 4 months (treatment or positive control group), 6 received fluvastatin (in addition to an HC diet) in the fourth month (statin group), and 6 rabbits were returned to normal chow in the last month (diet withdrawal group) after receiving 3 months of an HC diet. The remaining 4 atherosclerotic animals received cold (unlabeled) MPI before radiotracer administration to evaluate the specificity of radiotracer uptake.

Experimental atherosclerosis model. Male NZW rabbits (2.5 to 3.5 kg, Western Oregon Breeding Laboratories, Philomoth, Oregon) were started on a high-fat, HC diet containing 0.5% cholesterol and 6% peanut oil. One week later, balloon de-endothelialization of the abdominal aorta was performed with a 4-F Fogarty embolectomy catheter (12-040-4F, Edwards Lifesciences LLC, Irvine, California) as described previously (20). Briefly, animals were anesthetized with a mixture of ketamine and xylazine (100 mg/ml, 10:1 vol/vol; 1.5 to 2.5 ml subcutaneously). The right femoral artery was surgically exposed, and an embolectomy catheter was introduced through an arteriotomy site and advanced in the aorta up to the level of the diaphragm. The catheter was inflated to 3 psi and pulled antegrade to the bifurcation of aorta for endothelial denudation; 3 such denudation passes were made. After removing the catheter, the femoral artery was ligated, the incision site was closed, and the animals were returned to cages. The HC diet was continued for 16 more weeks. In 6 animals of the diet withdrawal group, normal chow was used in the last 4 of 16 weeks. In the 6 animals of the statin treatment group, fluvastatin (1 mg/kg orally, once per day, kind gift from Novartis Pharmaceuticals, Tokyo, Japan) was given for the last 4 of 16 weeks, as the animals continued to receive the HC diet. Blocking experiments were performed to evaluate the specificity of radiotracer for MMP. For this purpose, cold MPI was administered in 4 doses (0.02, 0.5, 1.0, and 2.0 mg/kg) intravenously 30 min before radiotracer administration for radionuclide imaging. This protocol

Table 1 Atherosclerosis and Control Animal Groups and Nature of Interventions

Group	Balloon De-Endothelialization	High-Cholesterol Diet	Intervention	n	Tracer	Purpose
Disease control	–	–	—	12	MPI	Negative control
Treatment control	+	+ (all 4 months)	—	18	MPI	Positive control
Statin intervention	+	+ (all 4 months)	Fluvastatin (4th month)	6	MPI	Effect of fluvastatin prescription
Diet withdrawal	+	+ (first 3 months)	Normal chow (4th month)	6	MPI	Effect of diet modification
Tracer control	+	+ (all 4 months)	—	4	Cold MPI before MPI imaging	Evaluation of specificity of MPI
Blood clearance	–	–	—	3	MPI	Tracer half-life

MPI = matrix metalloproteinase inhibitor.

follows the Guidelines for the Care and Use of Laboratory Animals established by the National Institutes of Health (NIH Publication No. 85-23, revised 1996) and was approved by the Institutional Laboratory Animal Care and Use Committee at the University of California, Irvine.

Targeting agent and radiolabeling. The targeting radiotracer, MPI, used in the present study comprises a technetium-99m–labeled broad-spectrum MMP-inhibiting macrocyclic compound, RP-805 (a kind gift from the Research and Development division of Bristol-Myers Squibb Imaging Inc., North Billerica, Massachusetts). The structure of MPI has been previously reported (21,22) and is shown in Figure 1. A portion of this compound binds to the exposed catalytic domain of MMP. On the basis of the enzymatic assays, MPI binds specifically to a broad range of active MMP and not to other proteases (Fig. 1), and shows an enzyme inhibitory profile (IC50) of 6.5, 14, <6.4, 7.4, <6.0, 7.3, 27, and 95 nM for MMP-2, -3, -7, -9, -12, and -13, and ADAM-10 and -17, respectively. For radiolabeling of MPI, the contents of the vehicle vial were dissolved in 0.5 ml of 0.9% sterile saline, and the clear solution was transferred to a vial containing 25 to 35 μg MPI. The mixture was incubated for 10 min, and then ~90 mCi/ml of Tc-99m pertechnetate was added to the solution. The reaction vial was heated at 100°C for 10 min. Finally, high-pressure liquid chromatography analysis was performed to check the radioefficiency, which showed a product peak of >97%. The radiotracer was intravenously administered to all animals through the marginal vein of the right ear.

Radionuclide imaging, protocol, and data collection. Radionuclide imaging was performed immediately after radiotracer administration and 4 h later using a dual-head micro-SPECT gamma camera coupled with micro-CT (X-SPECT, Gamma Medica, Inc., Northridge, California). The SPECT images of the aorta were acquired in a 64 × 64 matrix, 32 stops at 20 s (at 0 h) or 120 s (at 4 h) per stop at 140 keV photopeak of Tc-99m with 15% windows using a low-energy, high-resolution parallel-hole collimator. After SPECT acquisition, a micro-CT scan was acquired without having to move the animal. The micro-CT used an X-ray tube operating at 50 kVp and 0.6 mA. Images were captured for 2.5 s per view for 256 views in 360° rotation. The micro-CT images were transferred to a 256 × 256 matrix and micro-CT tomographic studies were fused, allowing scintigraphic and anatomic information in all tomographic scans in the 3 different spatial axes. After imaging, animals were killed with an overdose of sodium pentobarbital (120 mg/kg). The aortas were harvested for ex vivo gamma imaging. The entire aorta was then segmented at 1-cm intervals, weighed, and gamma counted in an automatic well-type gamma counter (PerkinElmerWallac Inc., Gaithersburg, Maryland) for calculation of the percent injected MPI dose per gram uptake in aortic tissue (%ID/g). Aorta

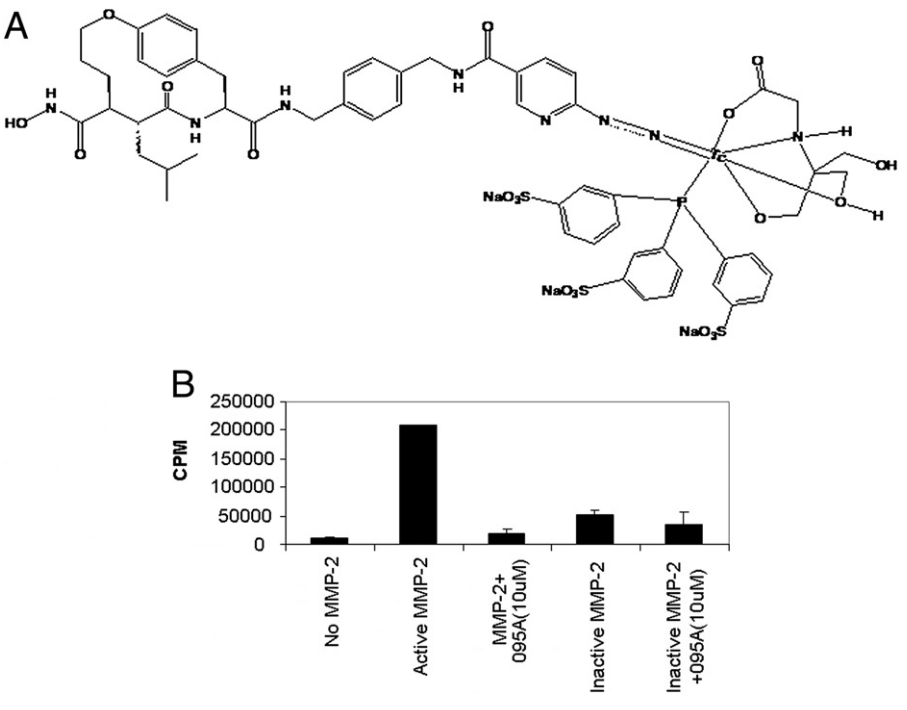

Figure 1 Structure and Specificity of MPI

(A) Structure of matrix metalloproteinase inhibitor (MPI) (Tc-99m–MPI). **(B)** Proof of the principle that the MPI used for radioimaging binds only to the active MMP. In this radioimmunoassay, radiolabeled MPI bound to active matrix metalloproteinase (MMP)-2 only.

was then processed for histologic and immunohistochemical characterization, and for MMP activity assays.

Blood clearance and biodistribution studies. In 3 unmanipulated normal rabbits, serial blood samples were drawn at 1, 5, 15, 30, 60, 90, 120, 150, and 180 min to obtain the blood clearance characteristic of the radiotracer. In addition, tissue samples of various organs were used for calculation of the %ID/g tissue uptake to characterize the nontarget organ biodistribution. To correct for the radioactive decay and permit calculation of the concentration of radioactivity as a fraction of the administered dose, aliquots of the injected dose were preserved and counted simultaneously.

Histological and immunohistochemical characterization. One-half of every 1-cm aortic segment was snap frozen and the other one-half was fixed overnight with 4% paraformaldehyde in phosphate-buffered saline (PBS, pH 7.4 at 4°C. Fixed tissue was stored in PBS/0.02% sodium azide (NaN_3) at 4°C until use. Each segment was subdivided into 3 equidistant sections, and dehydrated in a graded series of ethanol for paraffin embedding for further processing. Paraffin blocks were cut in 4-μm-thick sections on a microtome and floated on a water bath containing deionized water (43°C). The sections were then transferred to reagent-treated slides (Vectabond, SP-1800, Vector Labs, Burlingame, California), allowed to dry overnight, and stored at 4°C. To perform routine histologic studies, tissue sections were deparaffinized in xylene and graded series of ethanol. Tissue sections were stained with Movat pentachrome stains, and hematoxylin and eosin.

In atherosclerotic lesions, smooth muscle cells (SMC) were identified using a primary antibody against α-actin isotypes (MAB1420, 1:10,000, R&D Systems, Minneapolis, Minnesota) and macrophages were localized using a RAM-11 marker (M 0633, 1:3,000, DAKO, Carpinteria, California). For MMP characterization, monoclonal MMP-2 (gelatinase-A, IM53, 1:52,000, Calbiochem, Gibbstown, New Jersey); and monoclonal MMP-9 (gelatinase-B, IM37, 1:15,000, Calbiochem) antibodies were used. Immunohistochemical staining was performed using standard staining procedures as below. Tissue sections were deparaffinized, washed, and placed in a water bath for antigen retrieval at 90°C in (Vector Labs) antigen unmasking solution (H-3300) for 25 min followed by cooling to room temperature for 20 min. For α-actin and RAM-11 staining, sections were rinsed with PBS several times, and endogenous peroxidase quenched with fresh 3% H_2O_2 for 5 min. Tissue sections incubated in 2% immunoglobulin G–free, protease-free bovine serum albumin (001-000-161, Jackson, West Grove, Pennsylvania) with 0.1% Triton X-100 in PBS for 1 h to inhibit the nonspecific binding of primary antibody. Sections were incubated overnight with primary antibody at 4°C. After 3 washes, sections were subsequently incubated with biotinylated secondary antibody against the corresponding species of primary antibodies for 1 h at room temperature, followed by ABC treatment (PK-6100, Vector Labs). Primary and secondary antibodies were diluted in the same bovine serum albumin–containing blocking solution as described above. For staining of the MMP-2 and -9, the sections were pre-treated in water bath at 90°C and incubated with 0.005% pronase E for 10 min at room temperature. After washing in Tris-buffered saline, the sections were incubated overnight with primary antibody at 4°C, washed in Tris-buffered saline containing Tween 20, and treated with the catalyzed signal amplification II kit (DAKO) according to the manufacturer's instructions. Color reaction was developed using a Novared substrate-chromogen system (SK-4800, red color, Vector Labs) and diaminobenzidine kit (DAB, brown color, SK-4100, Vector Labs). The sections were counterstained with Gill hematoxylin. Sections incubated in parallel without primary antibody were used as quality control for staining procedure. Immunostaining was examined (Zeiss Axiovert-200 microscope, Carl Zeiss, Thornwood, New York), images were acquired (Zeiss Axiocam high-resolution digital color camera, 1,300 $\times$ 1,030 pixels, and Axiovision 3.1 software, Thornwood, New York), and digital images were analyzed (Image-Pro Plus version 5.0, Media Cybernetics, Bethesda, Maryland). The percent of immunopositive area (immunopositive area/total intimal area $\times$ 100) was determined for all markers by averaging several images per section that covered most to all of the plaque regions. Tissue samples from all regions of aorta and all animals were analyzed so that %ID/g MPI uptake and histologic severity of atherosclerotic lesions represented a broad spectrum, and allowed calculation of the correlation between MPI uptake and quantitative MMP distribution. All quantitative comparisons for a given marker were performed on sections stained simultaneously per group. Digital images were obtained using the same settings, and the segmentation parameters were constant within a range for a given marker and experiment.

MMP activity assays. Zymography was performed for the assessment of MMP-9 activity. Frozen plaque tissues were weighed and homogenized in 1 ml PBS containing 1% Triton X-100 and frozen overnight at −70°C. The next day, nondissolved fragments were removed by centrifugation at 12,000 rpm for 5 min and supernatant (with MMP) collected. The protein concentration was determined using a Lowry protein assay kit (Bio-Rad, Hercules, California). For each sample, 20-μg protein was loaded on 10% sodium dodecyl sulfate–polyacrylamide gel electrophoresis gel. The samples were run at 100 V per manufacturer's protocol (Novex, Carlsbad, California). After the run, the sodium dodecyl sulfate–polyacrylamide gel electrophoresis gel was renatured in the zymogram renaturing buffer for 1 h, followed by incubation in the developing buffer overnight. The gel was stained with Coomassie Blue and destained with 30% methanol/10% glacial acetic acid. The white bands with active MMP-9 were identified based on standards of purified recombinant activated MMP-9 and the molecular size. The optical density of the MMP-9 bands was quantified with ImageJ (Version 1.40, NIH, Bethesda,

Maryland) and expressed as a percentage of the control MMP-9 run on each gel sample.

The MMP-2 activity was measured by enzyme-linked immunosorbent assay using the Biotrak assay system (GE Healthcare, Piscataway, New Jersey). Supernatant with MMP, obtained as described above, was used in the assay. We incubated 200 μg of plaque protein overnight in 96-well plates containing MMP-2 antibody. On the next day, the plate was washed 4 times and 50 μl of the detection reagent was added. The plate was then read in a plate reader (Bio-Rad) at 405 nm. The level of active MMP-2 was quantified by using purified activated human MMP-2 as the standard.

Statistical analysis. All results are presented as the mean ± SD. To determine the statistical significance of differences between groups, 1-way analysis of variance was used; groups were compared independently using Fisher post-hoc least significant difference analysis. The correlation between radiolabeled MPI uptake and histological descriptors was determined by linear regression analysis. A value of $p < 0.05$ was considered statistically significant.

Results

Noninvasive imaging of MMP activity in atherosclerotic lesions. The Tc-99m–labeled MPI (6.9 ± 0.18 mCi) was administered intravenously for radionuclide imaging of atherosclerotic lesions. Immediately after tracer administration, blood pool images were obtained by micro-SPECT, which showed an aorta in front of a vertebral column localized by micro-CT image fusion. Serial image acquisition in the initial animals showed that the lesions could be visualized best at 3 to 4 h after tracer administration in atherosclerotic animals on an uninterrupted HC diet (Fig. 2). Initial blood pool images were observed similarly in control animals as well, but no tracer uptake in abdominal aorta was seen in these animals after 3 to 4 h (Fig. 2). The MPI uptake in delayed images was markedly reduced in the diet withdrawal group and in those treated with fluvastatin (Fig. 2). After imaging, animals were killed and the aortas were harvested for ex vivo gamma imaging. Ex vivo images of the explanted aorta showed intense MPI uptake in abdominal region of the atherosclerotic animals receiving an uninterrupted diet. Ex vivo images confirmed the in vivo imaging observations and correlated with gross distribution of pathologic lesions. No uptake was observed in the aortas obtained from unmanipulated, disease control rabbits receiving normal chow. The tracer uptake in ex vivo images was markedly reduced in the diet withdrawal and statin groups, again confirming the findings of in vivo imaging (Fig. 3). Maximum uptake was evident in the abdominal aortic region. Atherosclerotic lesions also were observed in the nondenuded arch and thoracic aortic regions in animals receiving an HC diet. As such, the radiotracer uptake in the arch of the aorta and thoracic aorta was also higher in animals receiving an uninterrupted diet compared with control animals.

Quantitative MPI uptake in aortic specimens and nontarget organs. After ex vivo imaging, 1-cm segments of the entire aorta were individually weighed and gamma counted for calculation of the %ID/g radio tracer uptake and the target-to-background uptake ratio. The MPI uptake in the abdominal atherosclerotic lesions of the uninterrupted diet group (0.10 ± 0.03%) was significantly higher than the uptake in abdominal aortic specimens from the control animals (0.016 ± 0.004%; $p < 0.0001$). The accumulation of MPI in atherosclerotic lesions was 6.3-fold greater than in the control animals. The MPI uptake decreased by 45% to 55% in the intervention groups; the quantitative uptake in statin (0.056 ± 0.011%; $p < 0.0005$) and diet withdrawal (0.043 ± 0.011%; $p < 0.0001$) groups was statistically significantly lower compared with the uninterrupted diet group (Fig. 3). To evaluate the specificity of radiotracer uptake for the MMP target, unlabeled MPI was administered 30 min before the radiotracer. There was a dose-related decrease in MPI uptake. Cold MPI administered in doses of 0.02, 0.5, 1.0, and 2.0 mg/kg reduced radiolabeled MPI uptake by 35%, 62%, 69%, and 86%, respectively. Radiolabeled MPI uptake after 2 mg/kg cold MPI was almost equivalent to radiolabeled MPI uptake in disease control normal rabbits (Fig. 3C). MPI uptake in various nontarget organs was also evaluated. The kidney showed the maximum radiation burden; %ID/g uptake in the cortex, medulla, and urine was 2.5 ± 0.4%, 0.11 ± 0.04%, and 0.47 ± 0.20%, respectively. All other organs showed minimal burden.

Pathologic characterization of atherosclerotic lesions. One-half of every 1-cm aortic segment was processed for histological analysis. Most of the atherosclerotic specimens from animals on an uninterrupted diet showed fibroatheromatous lesions. The neointimal lesions showed a high macrophage content, MMP-2 expression, and MMP-9 expression and a low SMC prevalence (Fig. 4). The macrophage content and the MMP expression were reduced markedly in the diet and statin intervention groups (Fig. 4). The percent macrophage area in the uninterrupted diet group (17.30 ± 8.17%) was significantly greater compared with the statin (5.77 ± 2.59%; $p < 0.001$) and diet withdrawal (2.16 ± 0.73%; $p < 0.0001$) groups (Fig. 5). On the other hand, there was an increase in the SMC prevalence in the intervention groups, particularly in the statin-treated group (Fig. 4). The SMC-positive area was significantly lower in the uninterrupted diet group (4.53 ± 1.89%) compared with the statin (17.72 ± 9.14%; $p < 0.0001$) and diet withdrawal (9.60 ± 4.92%; $p < 0.05$) groups (Fig. 5). Similar to macrophage prevalence, areas positive for MMP-2 and -9 were significantly greater in the uninterrupted diet group (4.80 ± 2.69% and 8.28 ± 3.85%, respectively) than in the statin (1.11 ± 0.69%, $p < 0.005$ and 3.45 ± 2.39%, $p < 0.005$, respectively) and diet withdrawal (0.97 ± 0.63%, $p < 0.0005$ and 2.32 ± 0.96, p

JACC Vol. 52, No. 23, 2008
December 2, 2008:1847–57

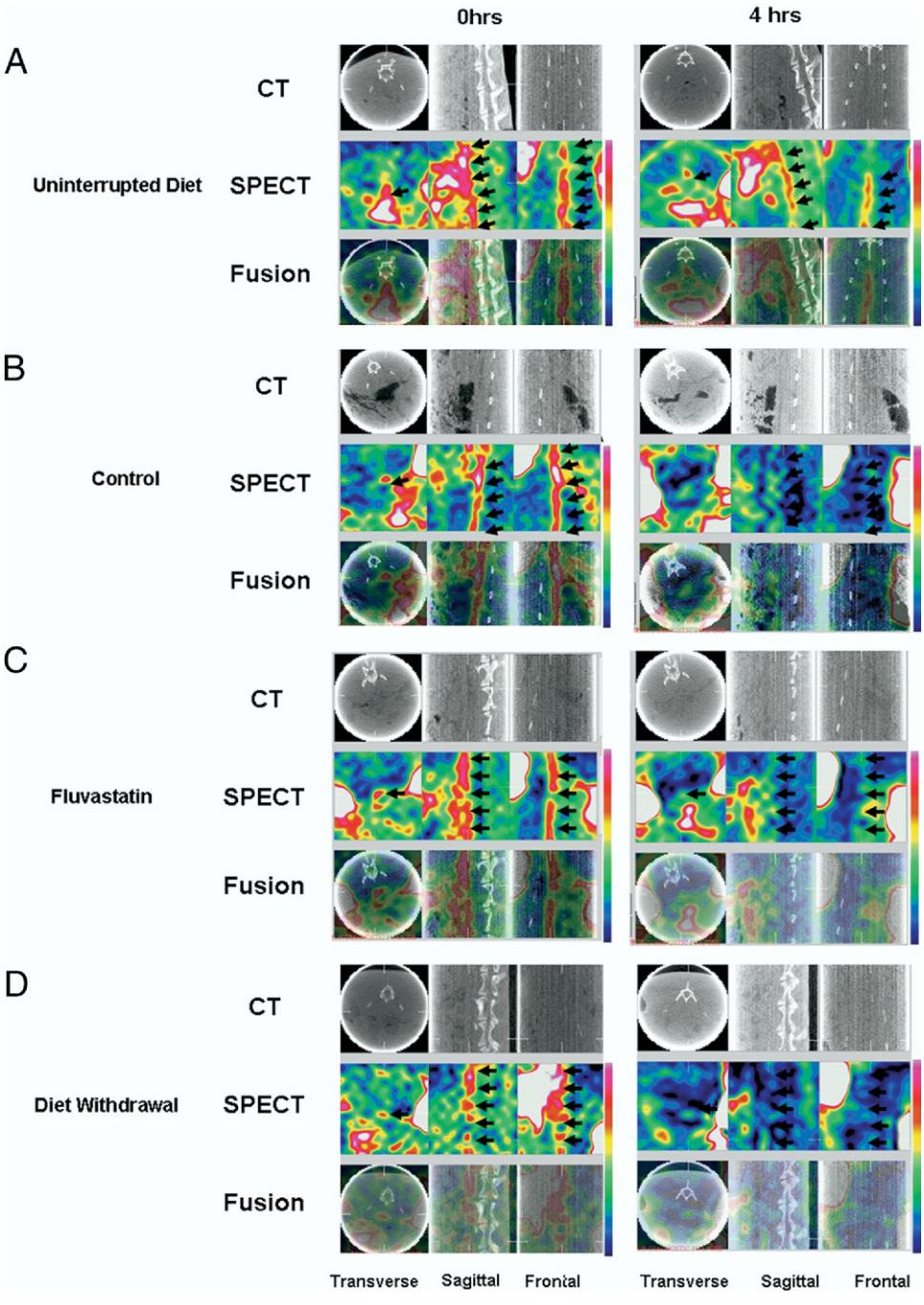

Figure 2 **Radionuclide Imaging of Atherosclerotic Lesions**

Images are presented in a 3 × 3 format in which **3 columns** display transverse, sagittal, and frontal projections, and **3 rows** display micro–computed tomography (CT), micro–single-photon emission computed tomography (SPECT), and fusion images. The **left set of 3 columns** displays images immediately (0 h) after radiotracer administration (representing blood pool image), and the **right set of 3 columns** displays images obtained at 4 h (representing tracer uptake in target tissue). Images obtained **(A)** from an atherosclerotic rabbit on uninterrupted diet, **(B)** from a control unmanipulated animal (with no atherosclerotic lesions), **(C)** from a fluvastatin-treated animal, and **(D)** after dietary modification. Blood pool **(left)** in all animals **(A to D)** can be observed **(arrows)** in front of vertebral column (as identified computed tomography and fusion images) in the early images. However, in delayed images **(right)** obtained at 4 h, radiotracer is cleared from the blood pool and uptake represents target tissue accumulation. Intense matrix metalloproteinase inhibitor (MPI) uptake is observed in an atherosclerotic animal on an uninterrupted diet **(A)**. No MPI uptake is discernable in a control animal **(B)**, statin-treated animal **(C)**, or after diet modification **(D)**.

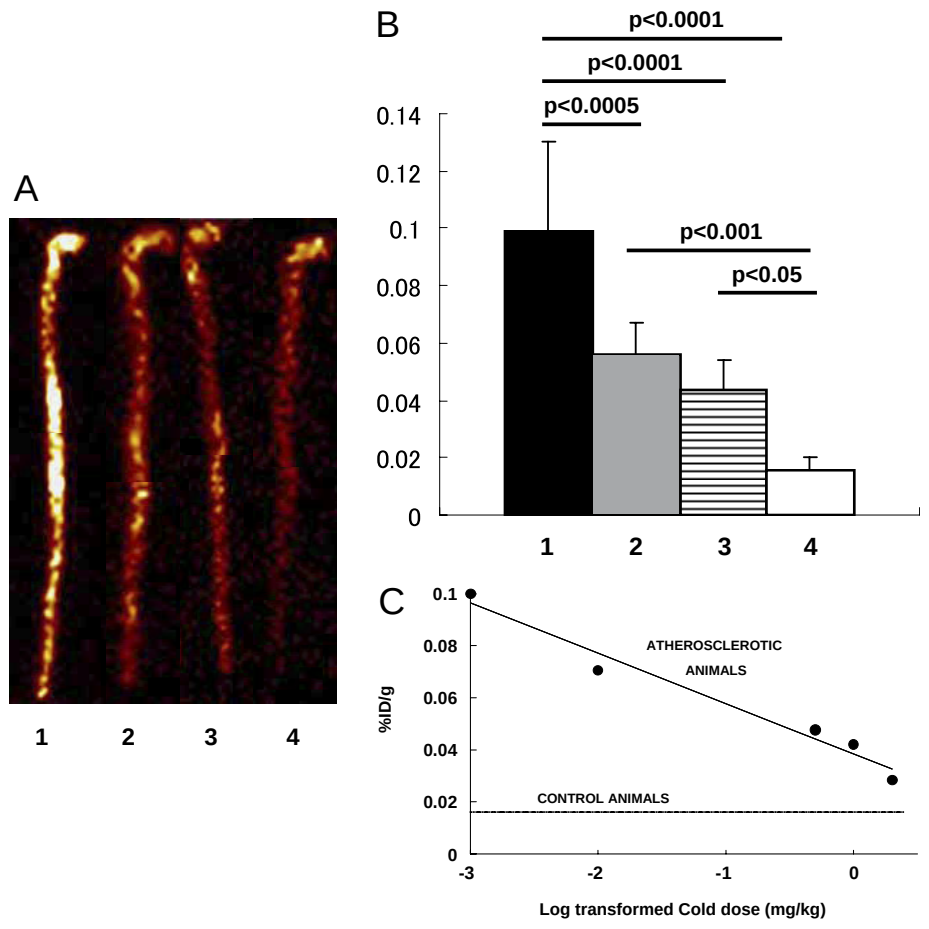

Figure 3 **Comparison of Radiotracer Uptake in the Aorta by Ex Vivo Imaging and Quantitative Estimates of MMP Activity as Expressed by %ID/g MPI Uptake**

(A) Ex vivo images of explanted aortas show intense matrix metalloproteinase inhibitor (MPI) uptake within abdominal aortas of rabbits receiving uninterrupted cholesterol diet for 4 months; uptake is significantly reduced in statin-treated and diet withdrawal animals, and no MPI uptake is observed in control animals. **(B)** Quantitative Tc-99m–MPI %ID/g uptake within abdominal aortas in various study groups. The MPI uptake was significantly lower in fluvastatin (**gray bar**, n = 6) and diet withdrawal (**lined bar**, n = 6) groups compared with the uninterrupted diet (**solid bar**, n = 18) group, and significantly higher than the control group (**open bar**, n = 12). No significant difference in MPI uptake was observed between statin and diet withdrawal groups. **(C)** Specificity of MPI radiotracer. Intravenous administration of increasing doses of cold (unlabeled MPI) 30 min before radiolabeled MPI progressively reduced radiolabeled MPI uptake in atherosclerotic lesions. %ID/g = percent total injected dose per gram of tissue.

< 0.001, respectively) groups (Fig. 5). Regression analysis showed a significant correlation between MPI uptake and expression of MMP-2 ($r = 0.542$, $p < 0.0001$) and MMP-9 ($r = 0.578$, $p < 0.0001$) (Fig. 5). There was also a significant direct relationship of MPI uptake with macrophage content ($r = 0.643$, $p < 0.0001$) but none with SMC content ($r = 0.082$, p = NS) (Fig. 5) in atherosclerotic lesions.

MMP activity in aortic fragments. The remaining one-half of each 1-cm aortic frozen segment was used for the assessment of MMP-2 and -9 activity. The level of active MMP-2 was significantly higher in the uninterrupted diet group (4.31 ± 0.78 ng/ml) compared with the control group (0.073 ± 0.101 ng/ml; $p < 0.0001$), and decreased significantly in the statin-treated (0.65 ± 0.44 ng/ml; $p < 0.0005$) and diet withdrawal (1.40 ± 0.93 ng/ml: $p < 0.001$) groups (Fig. 6). The zymography results also showed that the active MMP-9 levels were substantially increased in the uninterrupted diet group but decreased in the rabbits treated with fluvastatin or placed on a normal diet (Fig. 6). Quantitative analysis of the active MMP-9 in the uninterrupted diet group (313.3 ± 65.2%) was significantly greater compared with the control group (91.0 ± 46.6%; $p < 0.001$) (Fig. 6).

Discussion

The present study shows the feasibility of noninvasive radionuclide imaging of MMP activity in atherosclerotic lesions. The radiotracer uptake correlated with macrophage infiltration as well as with the expression and activity of MMP-2 and -9 activity. Histologically, plaques vulnerable to rupture usually show intense inflammation and the inflammatory cytokines induce expression of MMP (23–25). Macrophage-derived foam cells are the major source of

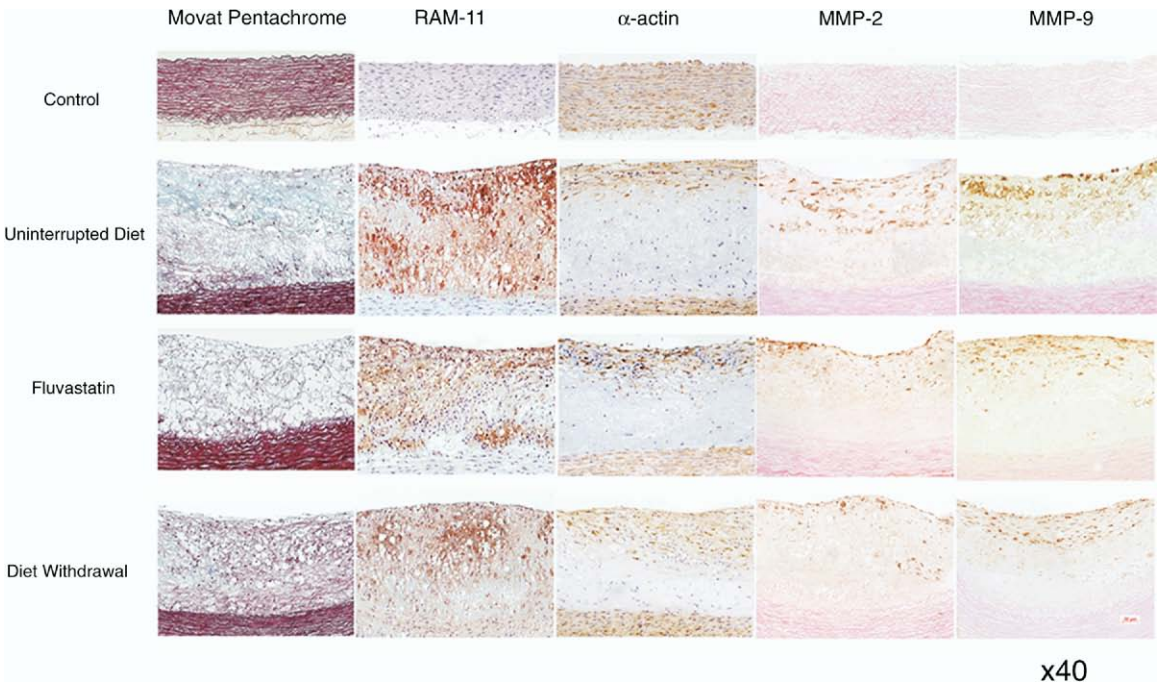

Figure 4 **Histopathological Characterization of Atherosclerotic Lesions in Various Experimental Groups**

Representative microphotographs from various groups are shown in **rows (from above):** control, uninterrupted diet, statin, and diet withdrawal groups. The **5 columns** represent **(from left)**: Movat pentachrome, RAM-11 (macrophage), α-actin (smooth muscle cell [SMC]), matrix metalloproteinase (MMP)-2, and MMP-9 immunostaining. Neointimal lesions in the uninterrupted cholesterol diet group showed high-macrophage, low-SMC, and high–MMP-2 and high–MMP-9 positive areas. In both the statin and the diet withdrawal groups, macrophage content and MMP-2 and -9 are significantly reduced, whereas SMC is increased. The control group has no neointimal thickening.

MMP expression in atherosclerotic lesions (5,26–28). Macrophages, when activated by cytokines such as tumor necrosis factor-α or interleukin-1, secrete inactive MMP, which is activated by plasmin or by inactivation of intrinsic inhibitors of MMP in tissue. The active MMP can degrade the connective tissue matrix. Both MMP mRNA and protein have been found in the fibrous caps in human atherosclerotic plaques, predominantly at the macrophage-rich shoulder regions (4,5,7,10,29–31), and may contribute to cap attenuation. Abundant expression of MMP-2 and -9 also is observed in positively remodeled human atherosclerotic arteries (9), which is associated with the presence of increased inflammatory cell prevalence and low collagen content in the neointima (32). The MMP inhibitors have been shown to retard expansive outward remodeling (33). Attenuation of fibrous caps and positive remodeling both contribute to plaque vulnerability.

The radiotracer uptake was substantially lower in animals after dietary modification and statin treatment and correlated with resolution of immunohistochemically verified MMP activation. It has been previously reported that expression of MMP-1, -2, -3, and -9 from macrophage cells or SMCs decreased with statin treatment (11–13,34,35). Statin treatment also reduced growth factor and proteolytic activity attributable to MMP-9 expression by human monocytes/macrophages in culture (11). Lipid lowering by dietary modification and statins has been shown to result in lower MMP activity in human carotid plaques by reducing macrophage prevalence (14). In addition to a decrease in collagenolytic activity, statins result in an increase in the SMC number and the expression of type I procollagen mRNA (13). A reduction in MMP activity could be one of mechanisms by which dietary modification and statin treatment reduce acute coronary events.

MMP-2 and -9 degrade fibrillar collagen after initial cleavage by MMP collagenases and may contribute to plaque rupture (31,36,37). Overexpression of MMP-9 in macrophages in advanced atherosclerotic lesions in apolipoprotein E knock-out mice has been shown to induce plaque rupture (38). In clinical studies, increased circulating MMP-2 and -9 have been reported in patients presenting with acute coronary syndrome but not in patients with stable angina (39). The MMP-9 levels also closely correlate with other circulating inflammatory markers associated with acute coronary events (40). Elevated MMP-9 levels have been prominently shown in unstable areas in carotid endarterectomy specimens (31). Accordingly, it has been proposed that MMP-9 levels may be a prognostic predictor for stroke or cardiovascular death (40,41). Additionally, MMP-2 degrades type IV collagen, which supports endothelium, and may underlie plaque erosion and hence acute coronary events (37,42). It is conceivable that noninvasive

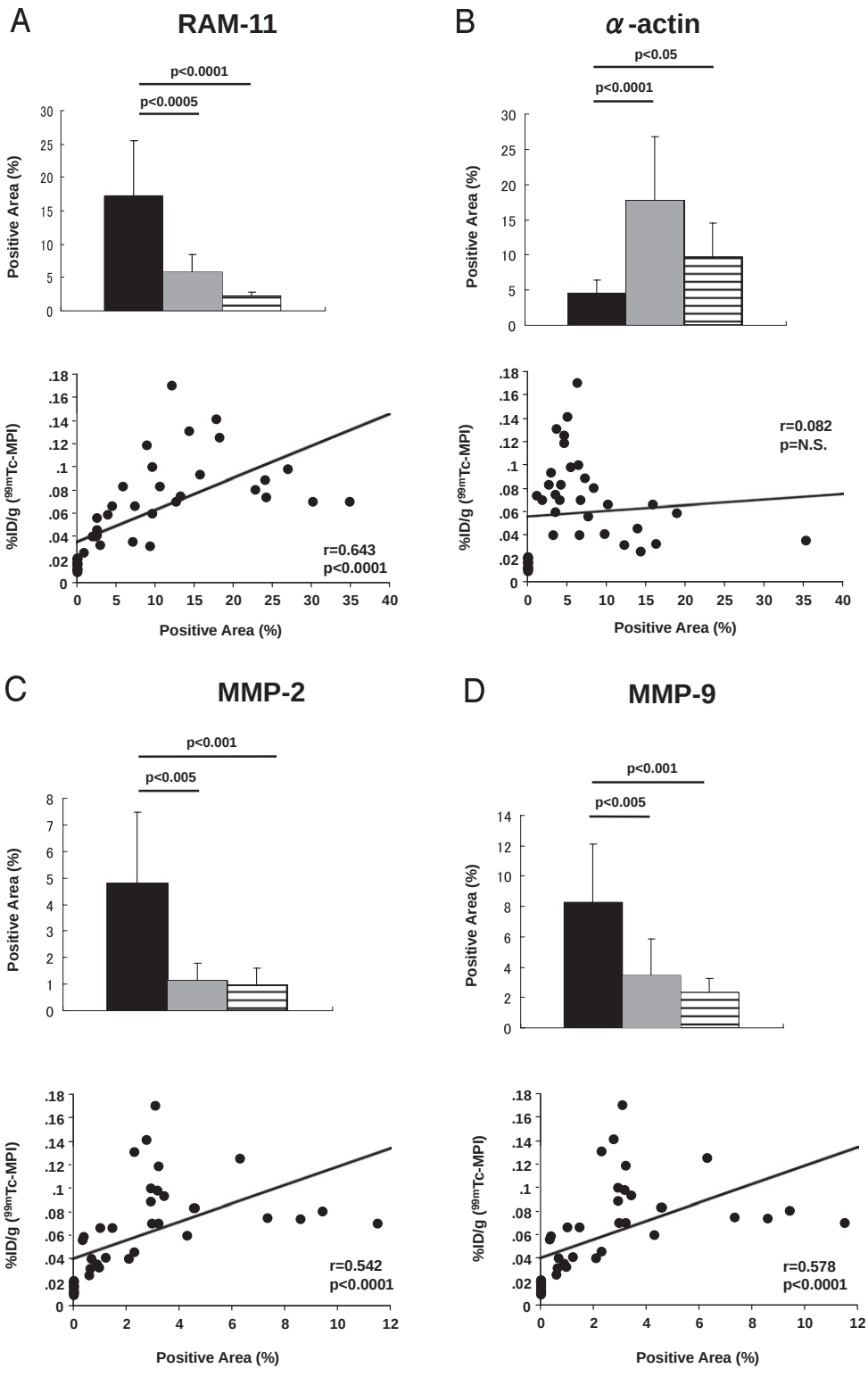

Figure 5 **Correlation of Macrophage, SMC, MMP-2, and MMP-9 Positive Areas With Quantitative MPI Uptake**

Macrophage **(A)**, SMC **(B)**, MMP-2 **(C)**, and MMP-9 **(D)** positive areas are presented as mean ± SD in uninterrupted diet (**solid bars**, n = 18), fluvastatin (**gray bars**, n = 6) and diet withdrawal groups (**lined bars**, n = 6) **(above)**. Intervention groups showed a significant decrease in immunopositive areas for macrophage compared with the uninterrupted diet group. In contrast, intervention groups showed a significant increase in immunopositive areas of SMC compared with the uninterrupted diet group. The MPI uptake correlated **(below)** significantly with the macrophage-positive area, but no correlation with SMC is apparent. Percent immunopositive areas for MMP-2 **(C)** and MMP-9 **(D)** decreased in intervention groups compared with the uninterrupted diet group. The MPI uptake correlated significantly with MMP-2 and -9 positive areas. Abbreviations as in Figure 4.

JACC Vol. 52, No. 23, 2008
December 2, 2008:1847–57

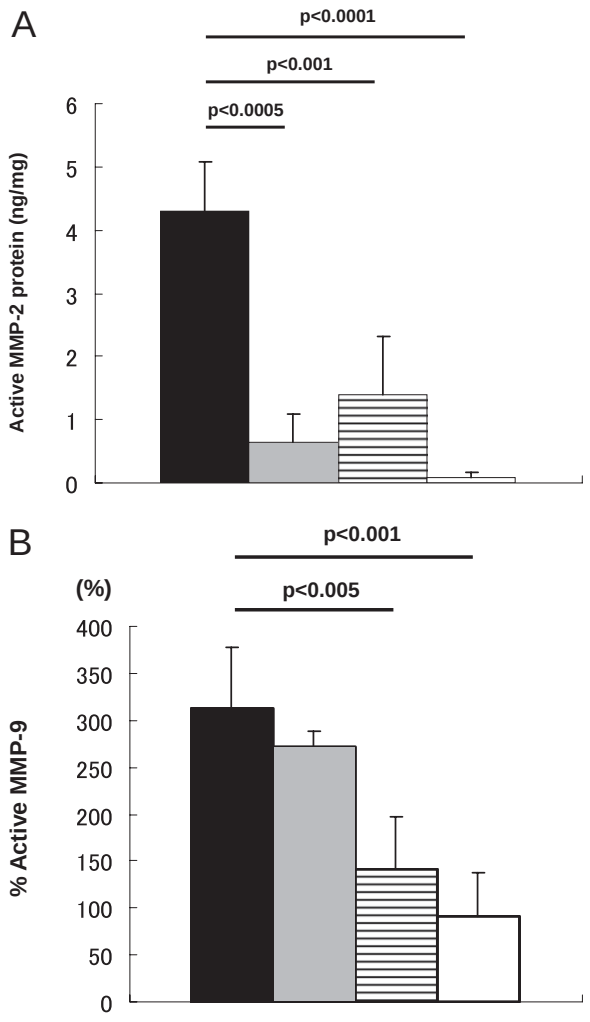

Figure 6 **MMP-2 and -9 Activity in Tissue Specimens From Various Animal Groups**

(A) The matrix metalloproteinase (MMP)-2 activity, represented as the mean ± SD of 3 individual samples by enzyme-linked immunosorbent assay, shows significantly higher levels in the uninterrupted diet group (**solid bars,** n = 3) compared with the fluvastatin (**gray bars,** n = 3) and diet withdrawal (**lined bars,** n = 3) groups and control (**open bars,** n = 3) animals. **(B)** The MMP-9 activity in aortas obtained from various animal groups was evaluated by zymography. The area of each band in gel zymograms was determined with ImageJ software to provide the net area value, and the change in area was calculated in comparison to the control active MMP-9 run in each gel (percent). The histogram represents mean ± SD of 3 separate experiments for each group. Results showed high MMP-9 levels in the uninterrupted group and a reduction in the intervention groups.

monitoring of MMP activity in the atherosclerotic plaque may address plaque vulnerability.

Conclusions

The present data show that in vivo quantification of MMP activity in atherosclerotic plaques is feasible by noninvasive targeted imaging. The radiotracer uptake correlates with the pathologically verified expression of MMP-2 and -9 in the plaque. The imaging observations also have reconfirmed previous observations that dietary modification and statin treatment may substantially decrease MMP activity in atherosclerotic lesions.

Reprint requests and correspondence: Dr. Artiom Petrov, Division of Cardiology, University of California, Irvine, Medical Science Building I, Room C-116, UCI Main Campus, Irvine, California 92697. E-mail: adpetrov@uci.edu.

REFERENCES

1. Davies M, Thomas A. Plaque fissuring: the cause of acute myocardial infarction, sudden death and crescendo angina. Br Heart J 1985;53:363–73.
2. Virmani R, Kolodgie FD, Burke AP, Farb A, Schwartz SM. Lessons from sudden coronary death: a comprehensive morphological classification scheme for atherosclerotic lesions. Arterioscler Thromb Vasc Biol 2000;20:1262–75.
3. Virmani R, Burke AP, Farb A, Kolodgie FD. Pathology of the vulnerable plaque. J Am Coll Cardiol 2006;47:C13–8.
4. Lendon CL, Davies MJ, Born GV. Atherosclerotic plaque caps are locally weakened when macrophages density is increased. Atherosclerosis 1991;87:87–90.
5. Galis ZS, Sukhova GK, Lark MW, Libby P. Increased expression of matrix metalloproteinase and matrix degrading activity in vulnerable regions of human atherosclerotic plaques. J Clin Invest 1994;94:2493–503.
6. Shah PK, Falk E, Badimon JJ, et al. Human monocyte-derived macrophage induce collagen breakdown in fibrous caps of atherosclerotic plaques. Potential role of matrix-degrading metalloproteinases and implications for plaque rupture. Circulation 1995;92:1565–9.
7. Sukhova GK, Schonbeck U, Rabkin E, et al. Evidence for increased collagenolysis by interstitial collagenases-1 and -3 in vulnerable human atheromatous plaques. Circulation 1999;99:2503–9.
8. Galis ZS, Khatri JJ. Matrix metalloproteinases in vascular remodeling and atherogenesis: the good, the bad, and the ugly. Circ Res 2002;90:251–62.
9. Pasterkamp G, Schoneveld AH, Hijnen DJ, et al. Atherosclerotic arterial remodeling and the localization of macrophages and matrix metalloproteinases 1, 2 and 9 in the human coronary artery. Atherosclerosis 2000;150:245–53.
10. Brown DL, Hibbs MS, Kearney M, Loushin C, Isner JM. Identification of 92-kD gelatinase in human coronary atherosclerotic lesions: association of active enzyme synthesis with unstable angina. Circulation 1995;91:2125–31.
11. Aikawa M, Rabkin E, Sugiyama S, et al. An HMG-CoA reductase inhibitor, cerivastatin, suppresses growth of macrophages expressing matrix metalloproteinases and tissue factor in vivo and in vitro. Circulation 2001;103:276–83.
12. Aikawa M, Rabkin E, Okada Y, et al. Lipid lowering by diet reduces matrix metalloproteinase activity and increases collagen content of rabbit atheroma: a potential mechanism of lesion stabilization. Circulation 1998;97:2433–44.
13. Fukumoto Y, Libby P, Rabkin E, et al. Statins alter smooth muscle cell accumulation and collagen content in established atheroma of Watanabe heritable hyperlipidemic rabbits. Circulation 2001;103:993–9.
14. Crisby M, Nordin-Fredriksson G, Shah PK, Yano J, Zhu J, Nilsson J. Pravastatin treatment increases collagen content and decreases lipid content, inflammation, metalloproteinases, and cell death in human carotid plaques: implications for plaque stabilization. Circulation 2001;103:926–33.
15. Tahara N, Kai H, Ishibashi M, et al. Simvastatin attenuates plaque inflammation: evaluation by fluorodeoxyglucose positron emission tomography. J Am Coll Cardiol 2006;48:1825–31.
16. Deguchi JO, Aikawa M, Tung CH, et al. Inflammation in atherosclerosis: visualizing matrix metalloproteinase action in macrophages in vivo. Circulation 2006;114:55–62.
17. Fujimoto S, Edwards DS, Zhou J, et al. Molecular Imaging of matrix metalloproteinase in atherosclerotic lesions: resolution with dietary modification and statin therapy. Circulation 2007;116:II 560.

18. Hartung D, Schafers M, Fujimoto S, et al. Targeting of matrix metalloproteinase activation for noninvasive detection of vulnerable atherosclerotic lesions. Eur J Nucl Med Mol Imaging 2007;34:S1–8.
19. Schafers M, Riemann B, Kopka K, et al. Scintigraphic imaging of matrix metalloproteinase activity in the arterial wall in vivo. Circulation 2004;109:r107–12.
20. Kolodgie FD, Petrov A, Virmani R, et al. Targeting of apoptotic macrophages and experimental atheroma with radiolabeled Annexin V: a technique with potential for noninvasive imaging of vulnerable plaque. Circulation 2003;108:3134–9.
21. Su H, Spinale FG, Dobrucki LW, et al. Noninvasive targeted imaging of matrix metalloproteinase activation in a murine model of postinfarction remodeling. Circulation 2005;112:3157–67.
22. Xue C, Voss M, Nelson D, et al. Design, synthesis, and structure-activity relationships of macrocyclic hydroxamic acids that inhibit tumor necrosis factor alpha release in vitro and in vivo. J Med Chem 2001;44:2636–60.
23. Van der Wal AC, Becker AE, van der Loos CM, Das PK. Site of intimal rupture or erosion of thrombosed coronary atherosclerotic plaques is characterized by an inflammatory process irrespective of the dominant plaque morphology. Circulation 1994;89:36–44.
24. Moreno PR, Falk E, Palacios IF, Newell JB, Fuster V, Fallon JT. Macrophage infiltration in acute coronary syndromes: implications for plaque rupture. Circulation 1994;90:775–8.
25. Varnava AM, Mills PG, Davies MJ. Relationship between coronary artery remodeling and plaque vulnerability. Circulation 2002;105:939–43.
26. Welgus HG, Campbell EJ, Curry JD, et al. Neutral metalloproteinases produced by human mononuclear phagocytes: enzyme profile, regulation and cellular differentiation. J Clin Invest 1990;86:1496–502.
27. Galis ZS, Sukhova GK, Kranzhofer R, Clark S, Libby P. Macrophage foam cells from experimental atheroma constitutively produce matrix-degrading proteinases. Proc Natl Acad Sci U S A 1995;92:402–6.
28. Galis ZS, Asanuma K, Godin D, Meng X. N-acetyl-cysteine decreases the matrix-degrading capacity of macrophage-derived foam cells: new target for antioxidant therapy? Circulation 1998;97:2445–53.
29. Nikkari ST, O'Brien KD, Ferguson M, et al. Interstitial collagenase-1 (MMP-1) expression in human carotid atherosclerosis. Circulation 1995;92:1393–8.
30. Li Z, Li L, Zielke HR, et al. Increased expression of 72-kd type IV collagenase in human aortic atherosclerotic lesions. Am J Pathol 1996;148:121–8.
31. Loftus IM, Naylor AR, Goodall S, et al. Increased matrix metalloproteinase-9 activity in unstable carotid plaques: a potential role in acute disruption. Stroke 2000;31:40–7.
32. Pasterkamp G, Schoneveld AH, van der Wal AC, et al. The relation of arterial geometry with luminal narrowing and plaque vulnerability: the remodeling paradox. J Am Coll Cardiol 1998;32:655–62.
33. Prescott MF, Sawyer WK, Von Linden-Reed J, et al. Effect of matrix metalloproteinase inhibition on progression of atherosclerosis and aneurysm in LDL receptor-deficient mice over expressing MMP-3, MMP-12, and MMP-13 and on restenosis in rats after balloon injury. Ann N Y Acad Sci 1999;878:179–90.
34. Luan Z, Chase AJ, Newby AC. Statins inhibit secretion of metalloproteinase-1, -2, -3, and -9 from vascular smooth muscle cells and macrophages. Arterioscler Thromb Vasc Biol 2003;23:769–75.
35. Bellosta S, Via D, Canavesi VN, et al. HMG-CoA reductase inhibitors reduce MMP-9 secretion by macrophages. Arterioscler Thromb Vasc Biol 1998;18:1671–8.
36. Galis ZS, Johnson C, Godin D, et al. Targeted disruption of the matrix metalloproteinase-9 gene impairs smooth muscle cell migration and geometrical arterial remodeling. Circ Res 2002;91:852–9.
37. Visse R, Nagase H. Matrix metalloproteinases and tissue inhibitors of metalloproteinase: structure, function, and biochemistry. Circ Res 2003;92:827–39.
38. Gough PJ, Gomez IG, Wile PT, Raines EW. Macrophage expression of active MMP-9 induces acute plaque disruption in apoE-deficient mice. J Clin Invest 2006;116:59–69.
39. Kai H, Ikeda H, Yasukawa H, et al. Peripheral blood levels of matrix metalloproteinase-2 and -9 are elevated in patients with acute coronary syndromes. J Am Coll Cardiol 1998;32:368–72.
40. Blankenberg S, Rupprecht HJ, Poirier O, et al. Plasma concentrations and genetic variation of matrix metalloproteinase 9 and prognosis of patients cardiovascular disease. Circulation 2003;107:1579–85.
41. Eldrup N, Gromholdt ML, Sillesen H, Nordestgaard BG. Elevated matrix metalloproteinase-9 associated with stroke or cardiovascular death in patients with carotid stenosis. Circulation 2006;114:1847–54.
42. Farb A, Burke AP, Tang AL, et al. Coronary plaque erosion without rupture into a lipid core: a frequent cause of coronary thrombosis in sudden coronary death. Circulation 1996;93:1354–63.

Key Words: matrix metalloproteinase ■ molecular imaging ■ atherosclerosis ■ HMG coenzyme reductase inhibitor.